Global impact of road traffic on atmospheric chemical composition and on ozone climate forcing

Ulrike Niemeier,[1] Claire Granier,[2,3] Luis Kornblueh,[1] Stacy Walters,[4] and Guy P. Brasseur[1,5]

[1] Automobile emissions are known to contribute to local air pollution and to photochemical smog in urban areas. The impact of road traffic on the chemical composition of the troposphere at the global scale and on climate forcing is less well quantified. Calculations performed with the chemical transport MOZART-2 model show that the concentrations of ozone and its precursors (NOx, CO, and hydrocarbons) are considerably enhanced in most regions of the Northern Hemisphere in response to current surface traffic. During summertime in the Northern Hemisphere, road traffic has increased the zonally averaged ozone concentration by more than 10% in the boundary layer and in the extratropics by approximately 6% at 500 hPa and 2.5% at 300 hPa. The summertime surface ozone concentrations have increased by typically $1-5$ ppbv in the remote regions and by $5-20$ ppbv in industrialized regions of the Northern Hemisphere. The corresponding ozone-related radiative forcing is 0.05 Wm^{-2}. In order to assess the sensitivity of potential changes in road traffic intensity, two additional model cases were considered, in which traffic-related emissions in all regions of the world were assumed to be on a per capita basis the same as in Europe and in the United States, respectively. In the second and most dramatic case, the surface ozone concentration increases by $30-50$ ppbv ($50-100\%$) in south Asia as compared to the present situation. Under this assumption, the global radiative forcing due to traffic-generated ozone reaches 0.27 Wm^{-2}.

1. Introduction

[2] With more than 500 millions automobiles and trucks operating in the world, road vehicles release considerable amounts of chemical compounds in the atmosphere. One of these compounds is carbon dioxide, which is produced in combustion engines and contributes to the greenhouse effect of the atmosphere. *Schultz et al.* [2004] estimate that surface traffic has increased the atmospheric CO_2 mixing ratio by 17.4 ppmv, which should have led to a radiative forcing of nearly 0.3 Wm^{-2}. Nitrogen oxides (NOx = NO + NO$_2$), carbon monoxide (CO), and volatile organic compounds (VOCs), which are also emitted by combustion engines, contribute to the photochemical production of ozone and other secondary pollutants. Ozone is a greenhouse gas, and an increase in its concentration should lead to additional radiative forcing. Changes in the oxidizing potential of the atmosphere (i.e., in the level of tropospheric OH) are expected to modify the lifetime of several compounds, including methane, which also affects greenhouse forcing. In addition, high levels of ozone in the atmospheric boundary layer can cause health problems to humans, damages to plants, and are expected to reduce crop productivity. Urban ozone pollution in industrialized regions is strongest during summertime when photochemistry is most active. Finally, aerosol particles, which are also directly released by automobiles and trucks, or are formed as secondary products of engine exhaust, affect visibility and are also detrimental to human health. As a result of their direct interactions with solar and terrestrial radiation, sulfate aerosols tend to cool the Earth's surface [*Ramaswamy et al.*, 2001], while soot leads to surface warming [*Jacobson*, 2001]. Indirect effects produced by aerosol particles and affecting the physical properties and lifetime of clouds need also to be taken into account.

[3] Since *Haagen-Smit*'s [1952] pioneering study of the mechanisms responsible for the formation of the Los Angeles smog, many studies have been conducted to assess the impact of automobile emissions on air pollution. Most of these studies have focused on regional aspects [see, e.g., *Brücher et al.*, 2000; *Reis et al.*, 2000; *Borrego et al.*, 2003; *Brandt et al.*, 2003; *Buron et al.*, 2004] including the impact

[1]Max Planck Institute for Meteorology, Hamburg, Germany.
[2]Service d'Aéronomie/L'Institut Pierre-Simon Laplace, Paris, France.
[3]Also at Cooperative Institute for Research in Environmental Sciences/NOAA Aeronomy Laboratory, Boulder, Colorado, USA.
[4]National Center for Atmospheric Research, Boulder, Colorado, USA.
[5]Now at National Center for Atmospheric Research, Boulder, Colorado, USA.

on health and public cost [*Colvile et al.*, 2000]. Other studies have investigated the global effects of surface traffic on tropospheric composition [*Valks and Velders*, 2001; *Köhler et al.*, 2001; *Granier and Brasseur*, 2003; *Matthes*, 2003; *Matthes et al.*, 2005]. The purpose of the present study is to perform a new and more detailed assessment of automobile impacts on ozone and its precursors under several scenarios used here for sensitivity purposes. In contrast to the earlier study of *Granier and Brasseur* [2003], the present model study conducted at higher spatial and temporal resolutions, accounts for the traffic related emissions of hydrocarbons, analyze in more detail the regional impacts of road traffic emissions, assess the impacts of automobiles on the global ozone budget and quantify the corresponding ozone climate forcing. Changes in the atmospheric concentrations of CO_2 and of the major types of aerosols are not considered here.

[4] We present in section 2 information on road traffic emissions and their global distribution. After a brief description of the chemical transport model (section 3), used to provide quantitative estimates of the impact of automobile traffic, we present in section 4 several emission model scenarios that are adopted to drive the model integration. In section 5, we analyze the results of the model simulations and provide some quantitative estimates of the impact of road vehicles on the chemical composition of the atmosphere and on radiative forcing. Some conclusions will be presented in section 6.

2. Road Traffic Emissions

[5] There has been a dramatic increase in surface traffic, and hence in air pollution, since the development of the automobile industry at the beginning of the 20th century. The transport of passengers ($1.2*10^{13}$ passenger-kilometers in 1990) and of freight ($6*10^{13}$ tons km in 1990) has been growing steadily over the last century, and is expected to grow further in the decades ahead. The number of cars and trucks available, their mean age and travel distance per vehicle, and therefore the level of pollution produced by road traffic vary considerably from country to country. For example, in the year 2000, the average number of automobiles (trucks in brackets) per 1000 inhabitants was 482 (325) in the United States, 508 (54) in Germany, 435 (116) in Canada, 469 (105) in France, 381 (53) in the United Kingdom, and 492 (158) in Japan (U.S. Department of transportation, available from http://www.fhwa.dot.gov/policy/ohim/hs02), while in 1998 the total number of vehicles per 1000 inhabitant was only 10 in China and 13 in India (UN statistics, available from http://www.cyberschoolbus.un.org/infonation).

[6] It is difficult to estimate how road traffic will evolve in the future. No reliable economically based scenarios for the next 100 years are available, so that several hypothetical cases will be considered. These will, for example, assess how the chemical composition of the global troposphere would change if the road traffic emissions per capita in world, and in particular in developing countries, reached the traffic emissions per person currently recorded in Europe or in North America. Although such scenario is unlikely to occur in the future, it allows assessing the sensitivity of the photochemical system to a very large perturbation.

[7] The contribution of road traffic to current global anthropogenic emissions is significant. On the basis of estimates for 1997 [*Olivier et al.*, 2003], automobiles and trucks release each year 3480 Tg of carbon dioxide, 9 Tg (expressed as N) of nitric oxide, 196 Tg of carbon monoxide and 36 Tg of nonmethane hydrocarbons (NMHC). This represents approximately 15%, 30%, 36% and 27% of the total anthropogenic emissions (excluding those associated with wildfires). These ratios are particularly high in Europe (20%, 39%, 69%, 39%), the United States (24%, 32%, 81%, 44%) and Japan (18%, 41%, 52%, 44%) for CO_2, NO, CO and VOCs, respectively. For comparison, the road traffic emissions adopted by *Matthes et al.* [2005] are 9 Tg N/yr, 237 Tg CO/yr, and 36 Tg NMHC/yr.

[8] Figures 1a and 1b show the global distribution of the total emissions for carbon monoxide and nitric oxide from the POET emission database [*Olivier et al.*, 2003] on a $1° \times 1°$ grid, and Figures 1c and 1d present the distribution of the road traffic emissions. What is immediately noticeable from Figure 1c are the hot spot regions, where the CO emission fluxes are larger than $5*10^{10}$ molecule cm^{-2} s^{-1}. These are located in Europe, the northeastern United States, California, southern Mexico, east and Southeast Asia, Japan and Korea, the southern tip of South Africa, and the densely populated urban areas of South America. The emission patterns of VOCs are characterized by geographic patterns that are similar to those of CO and NO.

[9] In the regions with high traffic density, including the eastern United States, California, central Mexico, eastern Brazil, western and eastern Europe, the Middle East, India, Southeast Asia, Japan, South Africa and southeast Australia, the NO emissions by road traffic (Figure 1d) are estimated to be in the range $(0.2–2) \times 10^{10}$ molecules cm^{-2} s^{-1}, which is a large contribution to the total NOx source (Figure 1b). Total NO emissions are of the order of $(1–6) \times 10^{10}$ molecules cm^{-2} s^{-1} near both U.S. coasts, in Europe, China and Japan, and of the order of $0.2*10^{10}$ molecules cm^{-2} s^{-1} in eastern Brazil, the Middle East, India, South Africa, and southeastern Australia. In the case of carbon monoxide, the emission associated with road traffic is typically $(6–40) \times 10^{10}$ molecules cm^{-2} s^{-1} in the eastern United States and California, in Europe, eastern Asia, and is of the order of $(1–6) \times 10^{10}$ molecules $cm^{-2} s^{-1}$ in the vicinity of the large urban areas of South America, South Africa, Australia, the Middle East, India and China. Again these values must be compared with the total CO emissions (Figure 1a), which are typically of the order of $(10–60) \times 10^{10}$ molecules cm^{-2} s^{-1} in the industrialized regions of North America, Europe and eastern Asia, and reach typically $(10–40) \times 10^{10}$ molecules cm^{-2} s^{-1} near the megacities of South America and Asia, and in the Middle East. In less industrialized regions, up to 80% of the CO emissions result from traffic (Figure 1e). In the industrialized areas of Europe and North America, 30% to 60% of the emissions of CO are due to traffic, while the contribution of traffic in 1997 was less than 20% in India and China.

3. Brief Model Description

[10] In order to assess the impact of road traffic emissions on the chemical composition of the troposphere, we use a global chemical transport model, named MOZART-2
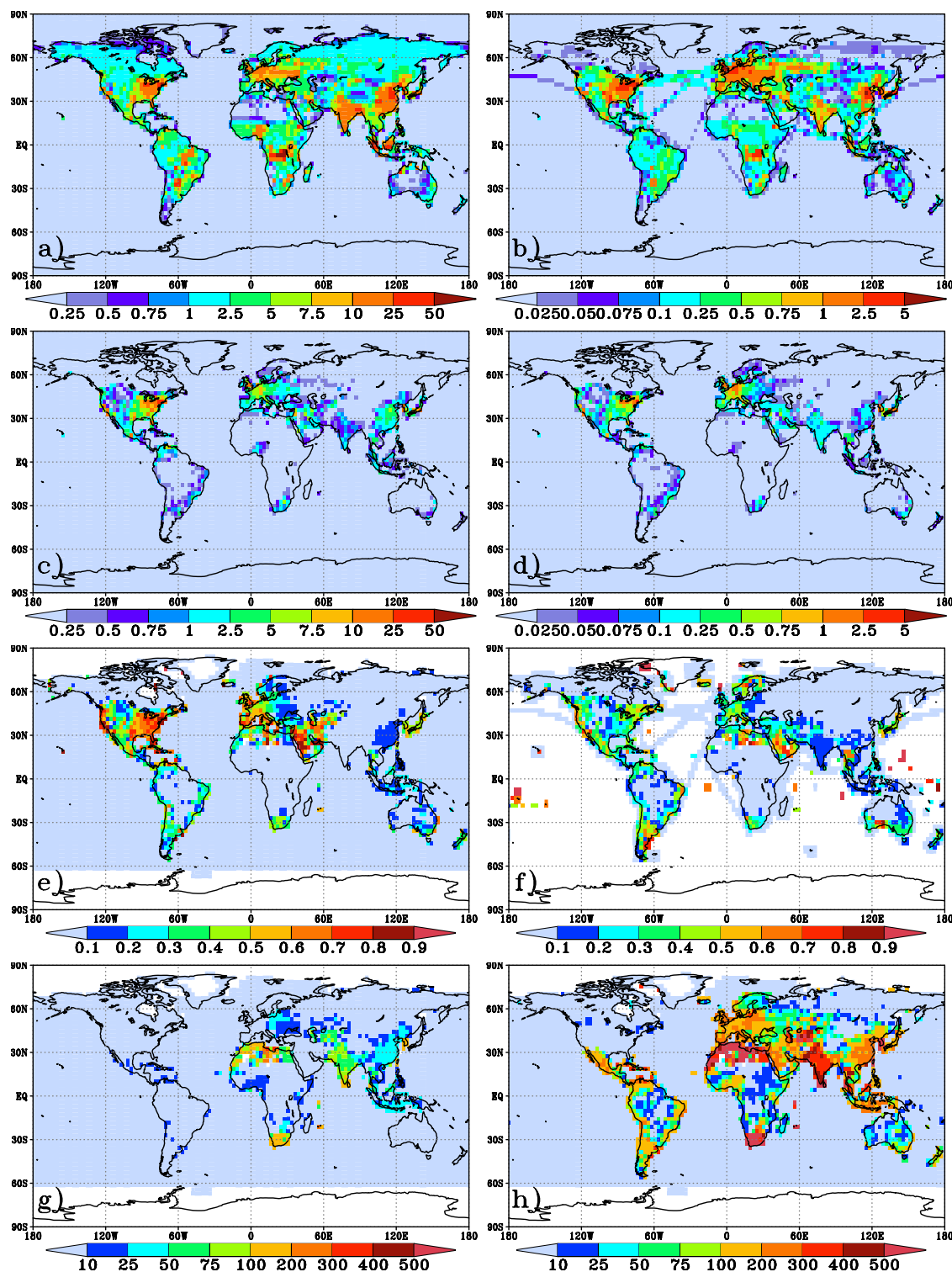
Figure 1. Distributions (in 10^{10} molecules cm^{-2} s^{-1}) of (a) CO and (b) NOx total emissions, (c) CO and (d) NOx emissions due to road traffic only, (e) CO road/total emission ratio, (f) NOx road/total emission ratio, (g) CO emissions difference (%) between cases 5 and 2 and (h) CO emissions difference (%) between cases 6 and 2. See text for further details.

(Model for Ozone and Related Tracers, version 2.1). MOZART-2 [*Horowitz et al.*, 2003] includes approximately 60 chemical species and 150 chemical and photochemical reactions, and specifically a detailed chemical scheme for tropospheric ozone, nitrogen oxides, and hydrocarbons. The

chemical mechanism describing the nonmethane hydrocarbons (NMHCs) includes ethane, propane, ethene, propene, isoprene, α-pinene (as a surrogate for all monoterpenes), and n-butane (as a surrogate for all hydrocarbons containing four or more carbon atoms, excluding isoprene and mono-

Table 1. Summary of Model Cases

Case Number	Case Description
1	no road traffic in the world
2	present worldwide traffic
3	same as 2 but with traffic emitting NOx only
4	no road traffic in North America
5	worldwide traffic as in western Europe
6	worldwide traffic as in United States

terpenes) as primary volatile organic species. Volatile aromatic compounds such as toluene, benzene and xylene, which are released by road vehicles [e.g., *Kristensson et al.*, 2004] and measured in urban and suburban areas [e.g., *Yamamoto et al.*, 2000; *Holzinger et al.*, 2001; *Batterman et al.*, 2002], are not explicitly accounted for (beside through the crude formulation of the surrogate compound). However, the sensitivity study conducted by *Matthes et al.* [2005] suggests that the impact of these compounds on tropospheric ozone should of the order of 3% only, and limited to specific confined regions.

[11] Tracer advection is performed using a flux-form semi-Lagrangian scheme driven by meteorological inputs every 6 hours. These are provided by the ECMWF operational meteorological analysis and forecasts for 1996 and 1997. Subgrid-scale convective and boundary layer parameterizations including dry and wet deposition are included in the model. Stratospheric concentrations of several long-lived species (including ozone) are constrained by relaxation toward climatological values.

[12] The model is integrated with a 20-min time step for the years 1996 and 1997. The horizontal resolution is approximately 2.8° in latitude and in longitude. This resolution is too coarse to represent the details of local effects, especially in the urban areas, where intense emissions are localized, and nonlinear effects associated with chemical reactions can be important. The resolution used in the study allows, however, to represent the long-range transport of chemical compounds within plumes produced in urban areas. The model extends to approximately 40 km (5 h Pa) altitude and includes 31 vertical levels. A more detailed description of the model is given by *Horowitz et al.* [2003].

[13] Surface emissions of nitrogen oxides, carbon monoxide and hydrocarbons include sources from fossil fuel combustion, biofuel and biomass burning, biogenic and soil emissions, as well as oceanic emissions. The database used in this study to derive the seasonal varying emissions is the so-called POET database for 1997, described by *Olivier et al.* [2003] and based on the EDGAR-3 inventory [*Olivier et al.*, 2001]. It provides global distributions of sources related to energy, surface traffic, chemical processes, waste, residential use, etc. at a horizontal resolution of $1° \times 1°$.

4. Model Scenarios

[14] The impact of road traffic on the chemical composition of the global troposphere is assessed by considering the different model cases summarized in Table 1. Some of these cases (1, 2, 3, and 4) are similar to those adopted by *Matthes et al.* [2005], which should facilitate the comparison of model results.

[15] Case 1 refers to a world with no emission from road vehicles. This case will be used as a reference to assess the impact of road traffic under different assumptions. Case 2 is intended to simulate the present situation, using road traffic emissions provided by *Olivier et al.* [2003]. The same conditions apply for case 3, but with the assumption that cars release NOx species only.

[16] In order to quantify the impact of North American vehicle emissions on the global composition, we consider case 4 in which the emissions of the United States and Canada are set to zero. We also assess the consequences of a hypothetical situation in which the automobile emissions per capita everywhere in the world would be the same as in western Europe (case 5, also called "European case") and as in the United States of America (case 6, also called "U.S. case"). For these two specific scenarios, the distribution of emissions related to traffic is calculated according to the values given in Table 2. In Table 2, the world is divided into 13 large areas. The population in these 13 areas is determined from the population distribution ($1 \times 1°$ resolution) provided by the Socioeconomic Data Applications Center (SEDAC) of the Center for International Earth Science Information [*Center for International Earth Science Information Network (CIESIN)*, 2000]. The traffic emissions are scaled in each area, so that the ratio between total emission and population is equal everywhere to the mean ratio observed in Europe (scenario 5) and in the United States (scenario 6). In case 5, however, the scaling is not applied in the areas covering the United States and Canada where the per capita emissions are considerably higher than in any other area of the world. Applying the European scaling factor in the United States and Canada would have led to a substantial decrease in the emissions of these two countries.

5. Model Results and Discussion

[17] In this section we assess the changes in the tropospheric composition in response to road traffic emissions as derived by the MOZART-2 model. We first successively consider the different cases described in the previous section and listed in Table 1. All figures show monthly mean values, calculated from instantaneous values collected at each model time step.

5.1. Global Impact of Current World-Wide Road Traffic

[18] In order to assess the impact of current automobile emissions on the composition of the global troposphere, we first compare the results of the model simulations performed under case 2 (current automobile traffic) and case 1 (no automobile traffic). For a better quantification of the photochemical mechanisms involved, we will also consider the special case labeled case 3, in which automobiles (current traffic) are assumed to release nitrogen oxides only.

5.1.1. Atmospheric Response in July

[19] We first discuss the response of the atmospheric composition to current world-wide automobile traffic for the month of July (Figures 2b and 3). In the case of carbon monoxide (CO), zonally average concentration at 50°N increases by almost a factor 1.2 in the boundary layer and 10–20% in the free troposphere of the Northern Hemisphere. In the tropics, where vertical exchanges by convective storms are intense, changes are noticeable up to the upper troposphere.

Table 2. Regional Traffic Emissions, Population and Resulting Ratios of Emissions per Capita Used for the Global European and U.S. Traffic Scenarios
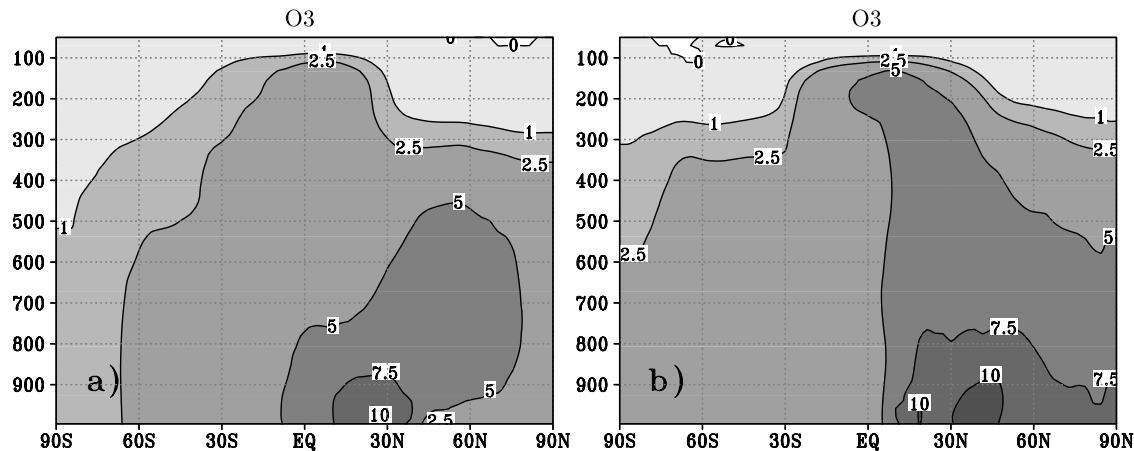
	Regional Emission, Tg CO/year	Population (in Millions) [CIESIN, 2000]	Ratio Total Emission/Population, kg CO yr^{-1} person^{-1}	European Case: Factor Applied to Emissions		U.S. Case: Factor Applied to Emissions	
				CO	NOx	CO	NOx
United States	69.3	267.7	259	1	1	1	1
Canada	6.0	31.0	193	1	1	1.3	0.8
South America[a]	22.2	474.7	46.9	1.2	1.9	5.5	3.8
Europe	21.9	384.3	56.7	1	1	4.5	2.0
Eastern Europe	3.2	119.7	26.4	2.1	3.4	9.8	6.9
FSU	7.2	292.1	24.7	2.3	5.2	10.5	10.6
Africa	8.9	701.3	12.7	4.5	7.4	20.3	15.1
Middle East	14.4	216.1	66.6	0.8	1.4	3.9	2.9
India	5.0	1248.4	4.0	14.2	10.6	64.4	21.6
China	19.3	1295.0	14.9	3.8	8.5	17.4	17.3
Southeast Asia	9.92	482.3	20.6	2.8	4.5	12.6	9.1
Japan	6.3	123.4	51.1	1.1	1.2	5.1	2.4
Oceania	2.0	30.9	63.8	0.9	0.6	4.1	1.3

[a]Note that Mexico is included in the "South America" region.

[20] When examining the spatial distribution of the CO changes calculated at the surface (Figure 3a), it is noticeable that the concentrations increase by 75–200 ppbv (50–150%) in urbanized/industrialized regions, including northeastern United States, California, Europe and eastern Asia. For example, in the vicinity of Washington, D. C., New York and Boston, the July CO mixing ratio changes from typically 200–250 ppbv in the absence of road traffic to 400–600 ppbv, when the emissions of vehicles are taken into account. A plume with enhanced concentrations of 30–40 ppbv (20–25%), produced by automobile emissions is visible over the North Atlantic. Carbon monoxide produced by road traffic is also transported from Europe to the Middle East. Increases of typically 50–100 ppbv (or about 50%) are visible over the Mediterranean (Figure 3a). A somewhat weaker plume originating from east Asia is also visible in the boundary layer over the North Pacific Ocean. The California source affects the western United States with a typical summertime CO increase of 50 ppbv or 50% when compared to the background levels. Concentration increases associated with automobile traffic in the areas close to South American and South African megacities are typically 20–

40 ppbv in the vicinity of Sao Paulo and Rio de Janeiro, 20–40 ppbv in the corridor between Santiago de Chile and Buenos Aires, and over 40 ppbv near Johannesburg. However, the maximum changes derived in the vicinity of densely populated areas are probably underestimated by the limited spatial resolution of the global model.

[21] In the case of surface NOx (Figure 3b), the largest absolute changes are taking place in the areas where the changes in carbon monoxide concentration are highest, with, however, less spatial dispersion around the source areas. The mixing ratio in these urbanized regions increases by about 0.5 to 10 ppbv (50–250%). Typical changes over the ocean far away from the source regions are of the order of 20% or smaller. In oceanic regions where NOx is enhanced as a result of intense ship traffic, the relative ozone response to continental automobile sources is less than 5%. An example of the geographical extent of the NOx plumes is provided by the situation in the vicinity of Hawaii, where dominant easterly winds transport the plume over the ocean west of the island. Somewhat more pronounced plumes are visible southeast of the South American continent and of Australia since during July (winter con-

Figure 2. Percentage change in the zonal mean concentration of ozone in (a) January and (b) July between a standard atmosphere and an atmosphere when no traffic emissions are considered (case 2–case 1).
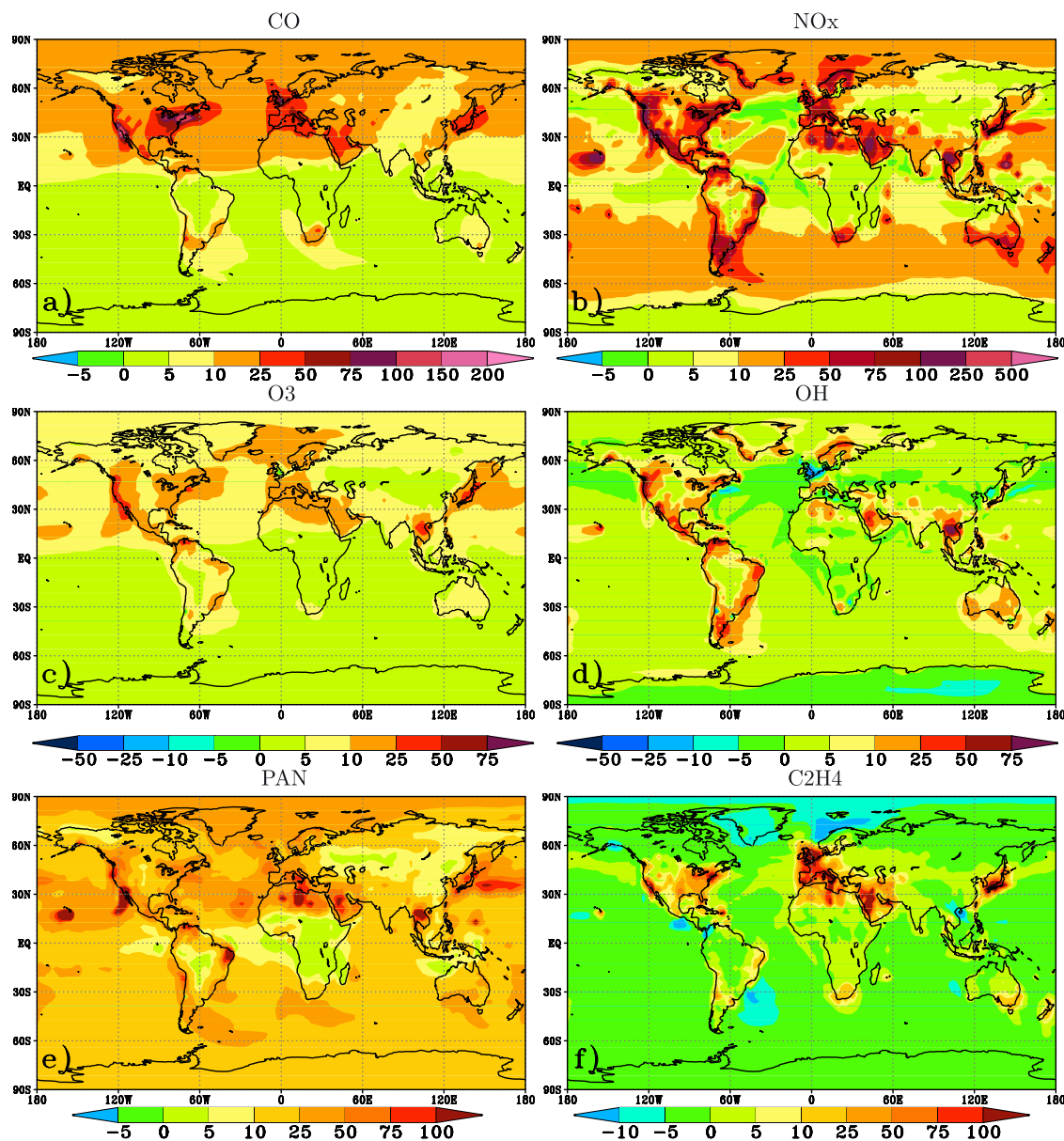
Figure 3. Percentage change in the July surface concentration (a) CO, (b) NOx, (c) ozone, (d) OH, (e) PAN and (f) C_2H_4 between a standard atmosphere and an atmosphere when no traffic emissions are considered (case 2–case 1).

ditions with reduced photochemical activity), the lifetime of NOx is longer than in the Northern Hemisphere.

[22] The changes in the zonally averaged concentration of peroxyacetyl nitrate (PAN) in July (not shown) produced by road traffic range from 10–15% in the tropics to 20–50% at higher latitudes in the Northern Hemisphere, especially in the summer polar region, highlighting the role of PAN as a reservoir species at low temperature. Changes of 10–20% are calculated in the Southern (winter) Hemisphere. Increases in the surface mixing ratio are largest in the urbanized/industrialized regions, where they reach 500 pptv to 1 ppbv (i.e., above 100%) (Figure 3e). Plumes of PAN are visible in similar areas as for NOx. When the emissions by automobiles are introduced in the model, the ratio of NOx to NOy concentration increases typically by 10–30% in source regions (air masses with fresh NOx), while the NOx to

PAN ratio increases by typically 10 to 25%. (the concentration of NOy is defined as the sum of the concentrations of $NO + NO_2 + NO_3 + HNO_3 + PAN + MPAN + 2*N_2O_5 + HO_2NO_2$.) The PAN to NOy concentration ratio decreases by 5–25% in the vicinity of urbanized and industrialized areas, and increases by 10–30% in the oceanic regions of the midlatitude Northern Hemisphere. Short-lived NOx is transformed by reactions with hydrocarbons into PAN, which is transported over longer distances, and decomposes in subsidence areas. PAN decomposition into NOx can therefore lead to increases in NOx concentrations in remote areas far away from road traffic sources.

[23] In the case of ethylene (C_2H_4), a hydrocarbon whose average surface mixing ratio is of the order of 100–200 pptv, its surface concentration (Figure 3f) can increase by more than 100% in urbanized and industrialized areas.

Table 3. Effect of Road Traffic Emissions on the Global Budget of Tropospheric Ozone

	January				July			
	Photochemical Production	Photochemical Destruction	Net Production	Surface Deposition	Photochemical Production	Photochemical Destruction	Net Production	Surface Deposition
No road traffic, Tg/month	474	461	12	60	507	456	52	81
With present-day cars, Tg/month	508	487	21	64	682	605	77	108
Percentage difference	7.3	5.7	66.5	1.8	34	33	47	33

[24] As shown by Figure 3d, the variations in the hydroxyl radical (OH) concentration, and hence in the oxidizing power of the atmosphere, are relatively localized in the vicinity of the regions where the NOx concentrations are substantially increased (e.g., coastal regions with intense urbanization). In these areas, local increases of $10-50\%$ are calculated for the concentration of OH. Further away from the sources, the perturbation in OH is either small, or can even become slightly negative (up to -10%), particularly along ship tracks and where CO plumes are noticeable. The sign in the OH perturbation is determined by the ratio between the intensities of NOx and CO perturbations. The first of these compounds has a lifetime in the boundary layer of only a few days (during summertime), so that its ability to convert HO_2 into OH is significant only close to the pollution sources. In the case of CO, whose lifetimes is about $1-2$ months in the summer boundary layer, long-distance transport occurs and OH can be destroyed even far away from the local sources. The changes in the zonally averaged OH concentration resulting from the extensive use of automobiles is also relatively limited. In July, the OH zonal mean concentration is enhanced by up to 5%.

[25] The calculated change in the zonally averaged ozone concentration resulting from road traffic during July (Figure 2b) is most pronounced in the Northern Hemisphere lower troposphere, where it reaches $5-10\%$ from $30°N$ to the summer pole. At about 5 km altitude in the free troposphere, it is typically $5-7\%$, and in the upper troposphere near 250 hPa, it ranges from 2 to 5% (or 2 to 10 ppbv). These later values can be compared to the ozone perturbations in the vicinity of the tropopause produced by the current fleet of commercial aircraft [Brasseur et al., 1998; Grewe et al., 2001; Penner et al., 1999]. In this case, the largest ozone perturbations occur at high latitudes, while in the case corresponding to road vehicles, the largest perturbations occur at low latitudes, where convective transport from the surface is most intense. The geographic distribution of the perturbation in the ozone concentration shows again the existence of hot spots in the urbanized areas (Figure 3c). Automobile traffic increases the ozone concentration in July by more than $5-10$ ppbv in North America, Europe, North Africa, east and south Asia, as well as in east Brazil, but reach more than 20 ppbv in the hot spots of California, northeastern United States, and 15 ppbv in the region of the Mediterranean. Expressed in relative amounts, automobile emissions enhance the summertime boundary layer ozone in the urbanized regions of the Northern Hemisphere by $20-40\%$, and by about 25% in the Mediterranean, 40% in southeast Asia and in California and 30% in Japan. Changes are also visible relatively far away from the sources. A plume with an ozone increase of 10% relative to background ozone can be seen in the northern Atlantic, while in the northern Pacific, a plume

formed in east Asia transports ozone toward the east. In the remote ocean boundary layer, the mean impact of road vehicles during July is $5-20\%$ in the Northern Hemisphere (summer) and less than 10% south of the equator (winter).

[26] Table 3 presents the global budget of tropospheric ozone calculated by the model, and shows how this budget is modified by the assumed emissions associated with road traffic. During July, when photochemical activity is largest in the most polluted regions of the Northern Hemisphere, the global photochemical production and destruction rates (as well as the surface deposition) are increased by a third of the values calculated in the absence of these emissions.

[27] The results for July are comparable to those of *Granier and Brasseur* [2003] with, however, more pronounced spatial gradients, an identification of pollution plumes and higher extreme values in the present model because of its higher spatial resolution. They are also similar to those presented by *Matthes* [2003] and *Matthes et al.* [2005], but, however, with some significant differences. For example, in July, the changes in the zonal mean surface concentrations of carbon monoxide and nitrogen oxides in both hemispheres are usually $20-30\%$ higher in the model of *Matthes et al.* [2005] than in the present study. At midlatitudes ($45°$), the resulting change in the ozone mixing ratio is 50% higher (15 versus 10 ppbv) in the Northern Hemisphere (summertime), but very similar (3.5 ppbv) in the Southern Hemisphere (wintertime).

5.1.2. Atmospheric Response in January

[28] During January, the change in the zonally averaged concentration of carbon monoxide resulting from automobile traffic is typically $20-30\%$ in the entire troposphere north of $30°N$. The corresponding increase in the NOx concentration reaches a maximum of 40% in the boundary layer near $45-60°N$ and decreases with height. The concentrations of PAN and C_2H_4 are enhanced by more than 25% and 50%, respectively in most of the winter northern extratropical troposphere. Both PAN and C_2H_4 show a stronger relative influence of traffic emissions than the other species, mainly because of their longer lifetime at low temperature and lower photolysis rates. The change in the ozone mixing ratio in the Northern Hemisphere is substantially lower in January (Figure 2a) (winter) than in July (summer), when stronger photolysis increases the formation of ozone. In the boundary layer, it is typically 2 to 5 pptv, which represents an increase of $5-8\%$, except near $20-30°N$, where it reaches a maximum of about 10%. In the free troposphere, the ozone increase reaches 7%. At 300 hPa, the winter ozone change is of the order of 2 ppbv or 2%. In the Southern Hemisphere (summer), the zonally averaged mixing ratio increases by 0.5 to 2 ppbv ($2-6\%$) at all tropospheric levels.

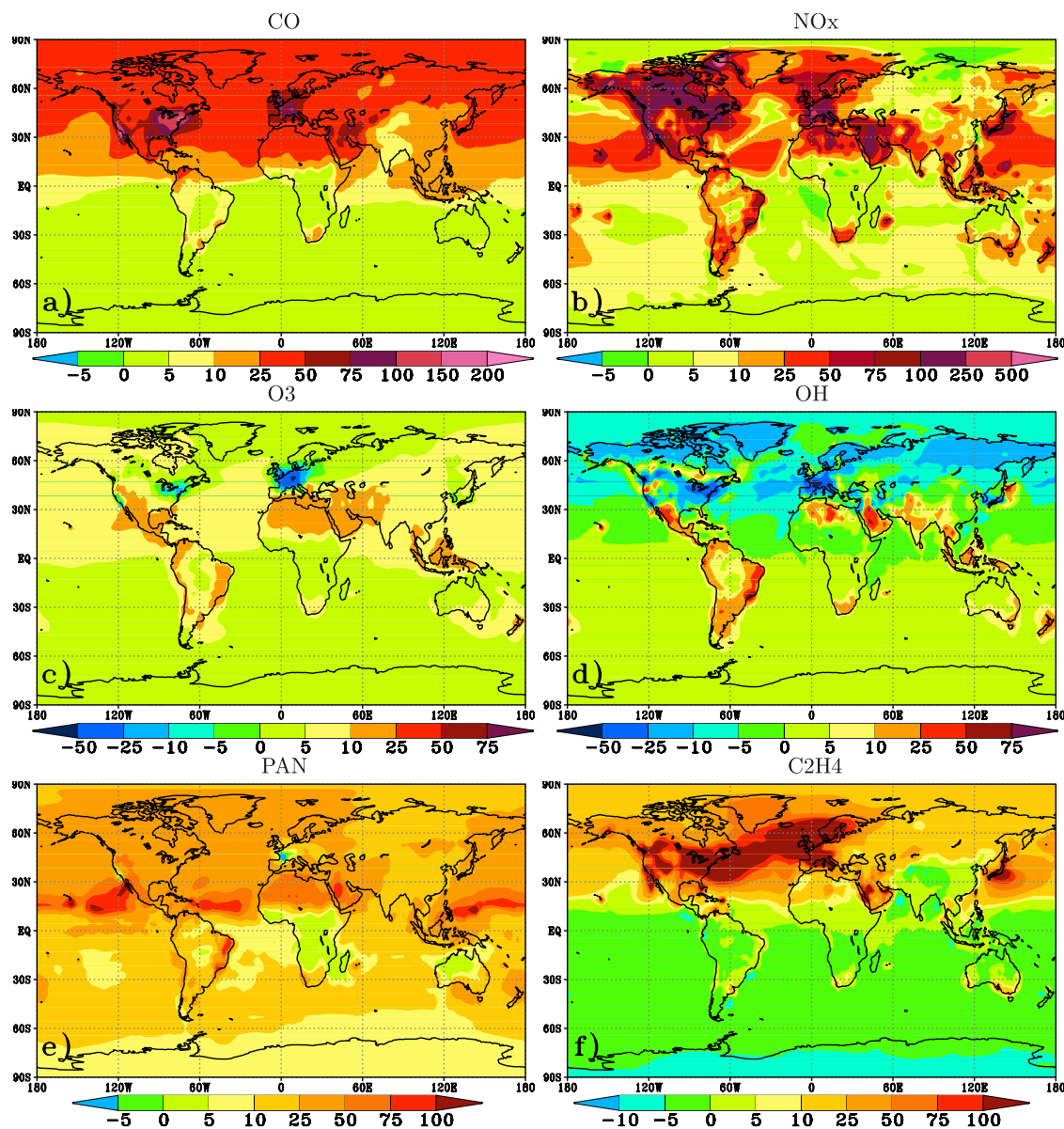[29] The changes in the near surface concentrations of chemical species in response to road traffic during the

Figure 4. Percentage change in the January surface concentration (a) CO, (b) NOx, (c) ozone, (d) OH, (e) PAN and (f) C_2H_4 between a standard atmosphere and an atmosphere when no traffic emissions are considered (case 2−case 1).

month of January are shown in Figures 4a–4f. In the Northern Hemisphere, the increase in the mixing ratio of CO during wintertime is approximately 50% larger than during summer, because of the larger lifetime of this gas. For example, outside urbanized/industrialized regions poleward of 30°N, the change in the CO mixing ratio resulting from road traffic is 25–50 ppbv, which represents more than 25% of the concentration calculated when automobile emissions are ignored. In the hot spots of the northeastern United States, California and Europe, the impact of road traffic exceeds 150 ppbv, which represents an increase of 75–150%. In the case of nitrogen oxides, automobile emissions increase the surface mixing ratio by more than 5 ppbv over the industrialized areas of the Northern Hemisphere (more than a doubling in the concentration), and by more than 10 ppbv (100%) over western Europe. In the Southern Hemisphere (summer), the calculated surface CO

concentration increases over the South American and African continents are typically 5–10 ppbv (or about 5%), a factor 2 less than during wintertime, and 10–100 pptv (5–25%) in the case of NOx.

[30] Substantial differences are noticeable between the near surface ozone changes calculated in January and July (see Figures 3c and 4c). For example, in Europe, the ozone concentration, which is increased by about 5–10 ppbv (20–30%) in summer, is reduced by approximately 10–15 ppbv (40–50%) during winter in response to road traffic. A similar, although somewhat smaller reduction is calculated over the northeastern United States (5 ppbv or 10–20%) and California. During winter, in the highly polluted industrialized and urbanized regions of the Northern Hemisphere, ozone is titrated, because of the high NOx concentration increases, and its surface concentration is reduced in response to road traffic. Outside these hot spots, downwind to
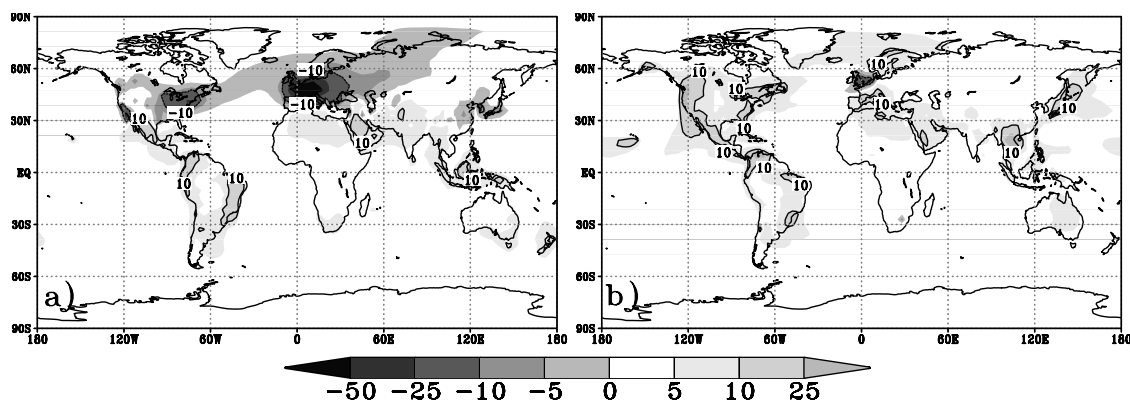
Figure 5. Percentage difference in the global ozone surface concentration due to road traffic in (a) January and (b) July when the road traffic is assumed to emit NOx only (case 3–case 1).

the north west, the changes in the concentrations are slightly positive (5%), with a further increases of the order of 2 to 5 ppbv (5–10%) north of 30°N, i.e., substantially less than during summertime. The largest increase is found in the latitudinal band around 20–30°N, where the radiation available for photochemical reactions is sufficiently high in January. Ozone increases of 2–10 ppbv (5 to 15%) are calculated in these regions.

[31] In the Southern Hemisphere (summer), the surface ozone concentration increases substantially in the vicinity of megacities (e.g., 5–10 ppbv or 20% near Sao Paulo), but only moderately outside these hot spots (Figure 4c). At many remote continental locations, the summertime changes in surface ozone concentrations (typically 2 ppbv) are smaller than during winter. This is explained by the fact that, far away from the emission regions, the summertime increase in NOx is smaller than in winter, and at the same time enhanced cloud cover, active convection and scavenging by precipitation during summer time in the subtropics slows down the photochemical production of ozone.

[32] Table 3 provides an estimate of the global ozone budget in January, and shows that the introduction in the model of the traffic emissions enhances the global photochemical ozone production and destruction by only 7.3 and 5.7%, respectively. The net photochemical production, however, is enhanced by 67%. When comparing our results with those of *Matthes et al.* [2005], significant differences are noted. At the surface, the midlatitude (45°), zonal mean ozone concentrations calculated in the present model during January are enhanced by 5 and 3.5% in the Northern (winter) and Southern (summer) hemispheres, respectively; they are enhanced by 10% in both hemispheres in the model of *Matthes et al.* [2005].

5.1.3. Traffic Emissions Limited to NOx

[33] As discussed in the previous sections, the formation of ozone by road vehicles is facilitated by the simultaneous emissions of nitrogen oxides, carbon monoxide and hydrocarbons. Catalytic converters installed on automobiles are more efficient in reducing CO than NOx emissions. In order to better understand the processes involved, and specifically assess the specific role of NOx emissions, we consider in this section the extreme (although unrealistic) case in which road traffic releases only nitrogen oxides. Case 3, which is considered here for sensitivity purposes, is therefore the same as case 2, but with the automobile emissions of CO

and hydrocarbons put equal to zero. Under these circumstances, the levels of CO and hydrocarbons (compared to a case in which the emissions by automobiles are ignored) are modified only by the changes in the atmospheric OH level produced by traffic-related NOx emissions.

[34] The geographical distribution in the ozone changes produced by this "NOx-only" perturbation (compared to a case without road traffic), is similar to the distribution of the changes calculated when all compounds emitted by automobiles are taken into account. The magnitude of the changes can, however, be substantially different (Figure 5). As in the case discussed in sections 5.1.1 and 5.1.2, the ozone mixing ratio tends to increase in response to traffic emissions, except in highly polluted areas (e.g., Europe), where ozone is titrated by nitrogen oxides. In January, the Northern Hemisphere (winter) change in ozone calculated in the NOx-only case is close to the ozone response derived when the emissions of all compounds are included in the model calculation. In the Southern Hemisphere (summer), however, the ozone response is somewhat lower in the NOx-only case (2–10 ppbv or 5–25% in South America and Australia) than in the comprehensive case. In July, the Northern Hemisphere (summer) surface ozone changes are also generally lower in the NOx-alone perturbation than if all emissions are considered. A negative response is even calculated over the UK. In the Southern Hemisphere (winter), the ozone changes are somewhat more pronounced in the NOx-alone scenario.

5.1.4. Radiative Forcing

[35] The radiative forcing associated with the ozone changes produced by road traffic (with all emissions included) includes two components, one related to the absorption of ultraviolet and visible solar radiation and one produced by the absorption of infrared terrestrial radiation. In both cases, the forcing is calculated as the monthly mean net flux difference at the tropopause between the cases in which automobile emissions are considered and in which they are ignored. The radiative forcing has been calculated using the ECHAM5 radiation scheme [*Roeckner et al.*, 2003] and the three-dimensional ozone field calculated by MOZART. No temperature adjustment is considered in response to the ozone-related change in the radiative flux.

[36] Figures 6a and 6b show the calculated tropopause forcing (solar plus terrestrial components) in January and July. During July, when the impact of automobile traffic is most pronounced, the change in the net flux ranges from
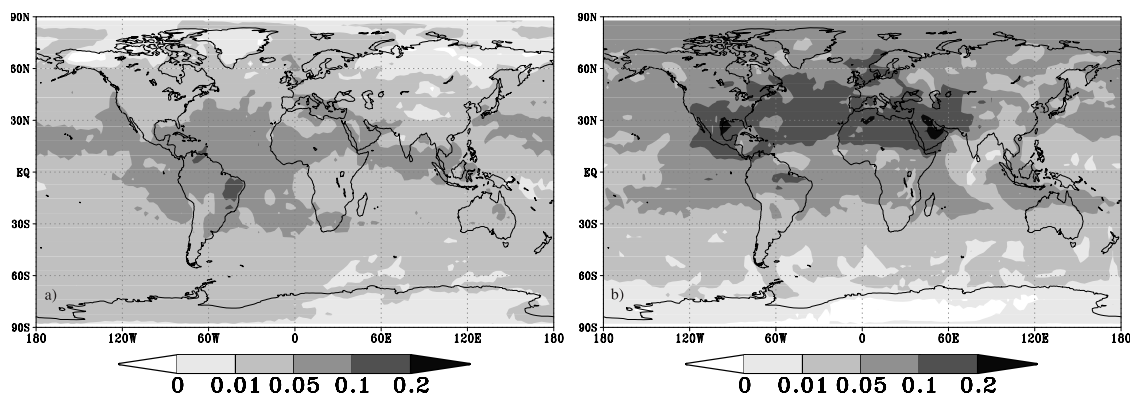
Figure 6. Tropopause radiative forcing in (a) January and (b) July resulting from ozone produced by road traffic.

0.05 to 0.2 Wm^{-2}, with the largest values located in a latitude band between 15° and 40°N. In the Southern Hemisphere (winter), the forcing varies between 0.01 Wm^{-2} at the edge of the Antarctic to 0.1 Wm^{-2} at the equator. The globally averaged ozone forcing produced by road vehicles in July is calculated equal to 0.05 Wm^{-2}. For January, the radiative forcing is considerably smaller at the global scale. The forcing can reach however values larger than 0.05 Wm^{-2} in the tropics. Maximum values of 0.1–0.2 Wm^{-2} are calculated near the equator. The globally averaged forcing in January is 0.03 Wm^{-2}. *Houghton et al.* [2001] gives a range of 0.28 to 0.43 Wm^{-2} for the global radiative forcing in response to ozone changes since the beginning of the industrialization. Thus road traffic emissions appear to be responsible for 10 to 20% of the total ozone radiative forcing.

5.2. Global Impact of North American Traffic

[37] As shown by Table 2, the ratio between traffic emissions and population is particularly high in the United States and in Canada. In this section, we assess the global impact of North American traffic emissions on the chemical composition of the atmosphere at the global scale. For this purpose, we consider a scenario (case 4) in which the traffic-related emissions of hydrocarbons, carbon monoxide and nitrogen oxides are set to zero over the North American continent, and we calculate the difference with the model case in which traffic is assumed to operate everywhere (case 2).

[38] Figure 7a and 7b shows the corresponding change in the CO and ozone concentration at the surface in July. When North American traffic emissions are set to zero, the summertime mixing ratio of carbon monoxide is reduced by more than 150 ppbv (or 50%) in the northeastern United States and California, and by 10–30 ppbv (10–20%) in the central United States (Figure 7a). In the entire Northern Hemisphere, the reduction in the CO mixing ratio amounts to more than 5 ppbv, and reaches more than 20 ppbv in a plume extending over the North Atlantic Ocean. In Europe, North Africa, the Middle East and Siberia, the reduction in the near surface CO resulting from the suppression of North American traffic is up to 10 ppbv (5%). In January (not shown), the reduction of CO is more substantial (e.g., 10–30% over the North Atlantic and up to 10% in Europe and east Asia). The change in the summertime surface NOx concentration is characterized by a reduction of 1–5 ppbv (20–50%) in the vicinity of the west coast of the United States and between the Mississippi and the east cost of North America, Away from the region where the traffic sources have been set to zero, the model calculates small changes in the NOx concentrations.
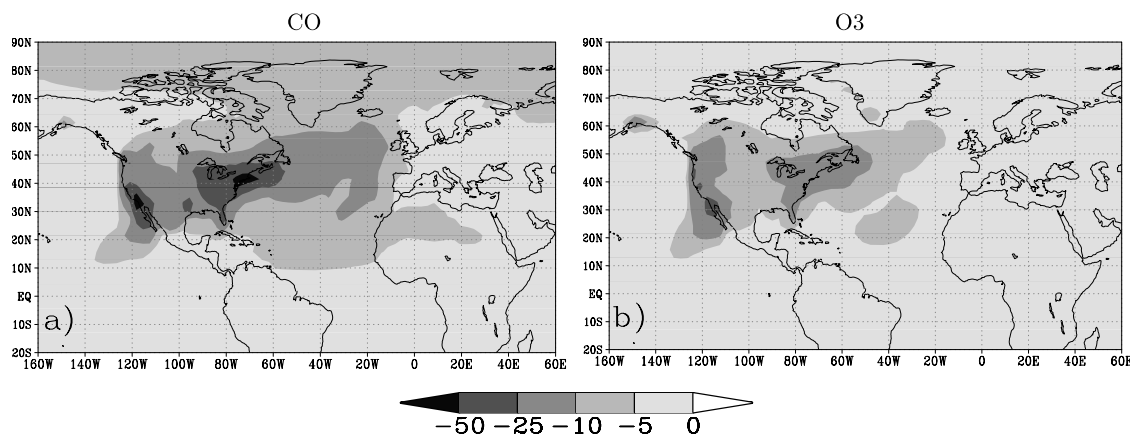

Figure 7. Percentage change in (a) CO and (b) ozone in July between current conditions and a case where traffic emissions are set equal to zero in North America (case 2–case 4).

[39] The reduction in the surface ozone concentration during July (Figure 7b) caused by the suppression of vehicles in North America is limited to 5% in most parts of the world, except in the northeastern United States and in California, where it reaches typically 10–20 ppbv (or 10 to 30%). In January (not shown), the changes in Northern Hemisphere surface ozone are smaller than in winter, and the suppression of road vehicle emissions leads even to an ozone increase (about 20%) in the region of the Great Lakes and in Northern California.

5.3. Impact of Enhanced Road Traffic

[40] In order to assess the impact of possible changes in road traffic intensity on the chemical composition of the atmosphere, we consider two additional model cases with different scenarios for vehicle emissions. These cases are not chosen to provide realistic predictions of future chemical perturbations, but to perform sensitivity tests that account for possible emission trends in the future. These cases refer to current tendencies in developing countries such as China, where the amount of cars has doubled between 1995 and 2000.

[41] In the first case (labeled case 5 in Table 1), the current traffic-related emissions of hydrocarbons, carbon monoxide and nitrogen oxides are scaled in each country, so that the emission rate per capita is the same as in western Europe (Table 2). In this case, the total amount of carbon monoxide, for example, emitted by road traffic is in the same range as the one used by *Brasseur et al.* [2006] for 2050 (A2-scenario) and based on the estimates of *Olivier et al.* [2003]. In the United States and Canada, where the emissions per inhabitant are higher than in Europe, the emissions are assumed to remain unchanged from their current values. In this particular simulation, the global emissions produced by road vehicles are 381, and 25 Tg/yr in the case of CO, and NOx (as N), respectively. Figure 1g shows the difference in the emissions of carbon monoxide applied in different regions of the world for this particular case. The largest changes occur in regions with high population densities and low GNPs. Changes in the road emissions are typically 20 to 50% (5 to 20 molecules $cm^{-2} s^{-1}$) in China 50 to 100% (10–20 molecules $cm^{-2} s^{-1}$) in India, 100 to 200% (1 to 10 molecules $cm^{-2} s^{-1}$) in North and South Africa, 10 to 50% (2 to 5 molecules $cm^{-2} s^{-1}$) in Southeast Asia and up to 25% (0.5 molecules $cm^{-2} s^{-1}$) in South America. A slight reduction in the emissions is applied in the Gulf States and in Australia.

[42] Under the adopted scenarios, as expected, the change in surface CO mixing ratio (Figure 8a) is small in the United States and over the North Atlantic (about 20 ppbv in January, less than 10 ppbv in July), but it reaches substantial values in India and China (300 ppbv in January, 100–200 ppbv in July or 10–50%). Large changes are also predicted in eastern Europe (100 ppbv in January, 20 ppbv in July) and in South Africa. The geographical extent of these perturbations is larger in winter (long CO lifetime) than in summer. Similar patterns are derived for NOx, with concentration increases in January (averaged over model grid cells, i.e., $2.8 \times 2.8°$) reaching approximately 20 ppbv (or 100–200%) in China and India, and 15 ppbv (50–100%) in eastern Europe. In July (Figure 8c), the maximum increase is close to 5 ppbv in the same areas. The change in

surface ozone during January (not shown) is characterized by a stronger titration by NOx and hence a reduction in the O_3 mixing ratio in eastern Europe (10 ppbv or 30%), Korea (15 ppbv or 50%). At the same time, the ozone mixing ratio increases by 10–30 ppbv (30–50%) in India, northern China and South Africa. In July (Figure 8e), the changes in the ozone surface mixing ratio are slightly positive (up to 10%) in most parts of the world. In India and China, however, an ozone increase of 10–30 ppbv (30–50%) is noticeable, while in North Africa, the mixing ratio is enhanced by 5–15 ppbv (10–30%).

[43] An extreme scenario (case 6), in which the emissions are scaled globally to the emissions per capita in the United States rather than of western Europe is also considered for sensitivity purposes. The difference in the emissions of carbon monoxide applied in different regions of the world for this particular case is shown in Figure 1h. Under these assumptions, the applied perturbation is globally higher than in case 5, with the total road traffic emissions being 1467 Tg/yr of carbon monoxide and 48 Tg N/yr of nitrogen oxides.

[44] The response to this chemical forcing is substantial. In January (NH winter, not shown), for example, the CO mixing ratio is enhanced by more than 100 ppbv (60%) in most locations of the Northern Hemisphere extratropics, with concentration increases of more than 300 ppbv (100–300%) in most parts of Europe and Asia, and in Mexico. In July (NH summer, see Figure 8b), the calculated changes in Northern Hemisphere surface CO are smaller, but remain larger than 50 ppbv north of 30°N, and over the Middle Atlantic. In western Europe (including the Mediterranean), India, China, and South Africa, the change in the CO mixing ratio can be larger than 300 ppbv (100–250%). In the case of NOx, the calculated concentration changes are also larger in winter than in summer. In January, they reach 30 ppbv in Europe, India, east Asia and North Africa, and 5 ppbv in South Africa and in the regions of the South American megacities. In July (Figure 8d), they are typically 1 to 10 ppbv in Europe, Mexico, the Mediterranean coast of Africa, South Africa, the Gulf States, India, east and Southeast Asia and Japan. In relative terms, these changes represent increases of approximately 25–75% in Europe, but as much as 500% in North and South Africa, in India, Southeast Asia and in Mexico. The slight decrease in the NOx concentration over North America is caused by decreased NOx emissions in Canada in the simulation (see Table 2).

[45] The change in surface ozone resulting from the adopted scenario (case 6) is characterized by a substantial increase at all latitudes of the Northern Hemisphere during wintertime (not shown), with some exceptions for the urbanized and industrialized hot spots of Europe and Asia. In the North American sector, where emissions of ozone precursors have not been changed, a small increase of 5–10 ppbv (10–20%) is predicted. Here, the titration of ozone by nitrogen oxides is intense in January, and the ozone mixing ratio is reduced by up to 10 ppbv (10–50%) in Europe and 20 ppbv (60%) in east Asia (specifically in Korea). In south Asia, the ozone mixing ratio increases by over 50 ppbv (70%), while in South Africa and both coasts of South America (where summer conditions prevail), the ozone concentration increases by about 25 ppbv and 5–
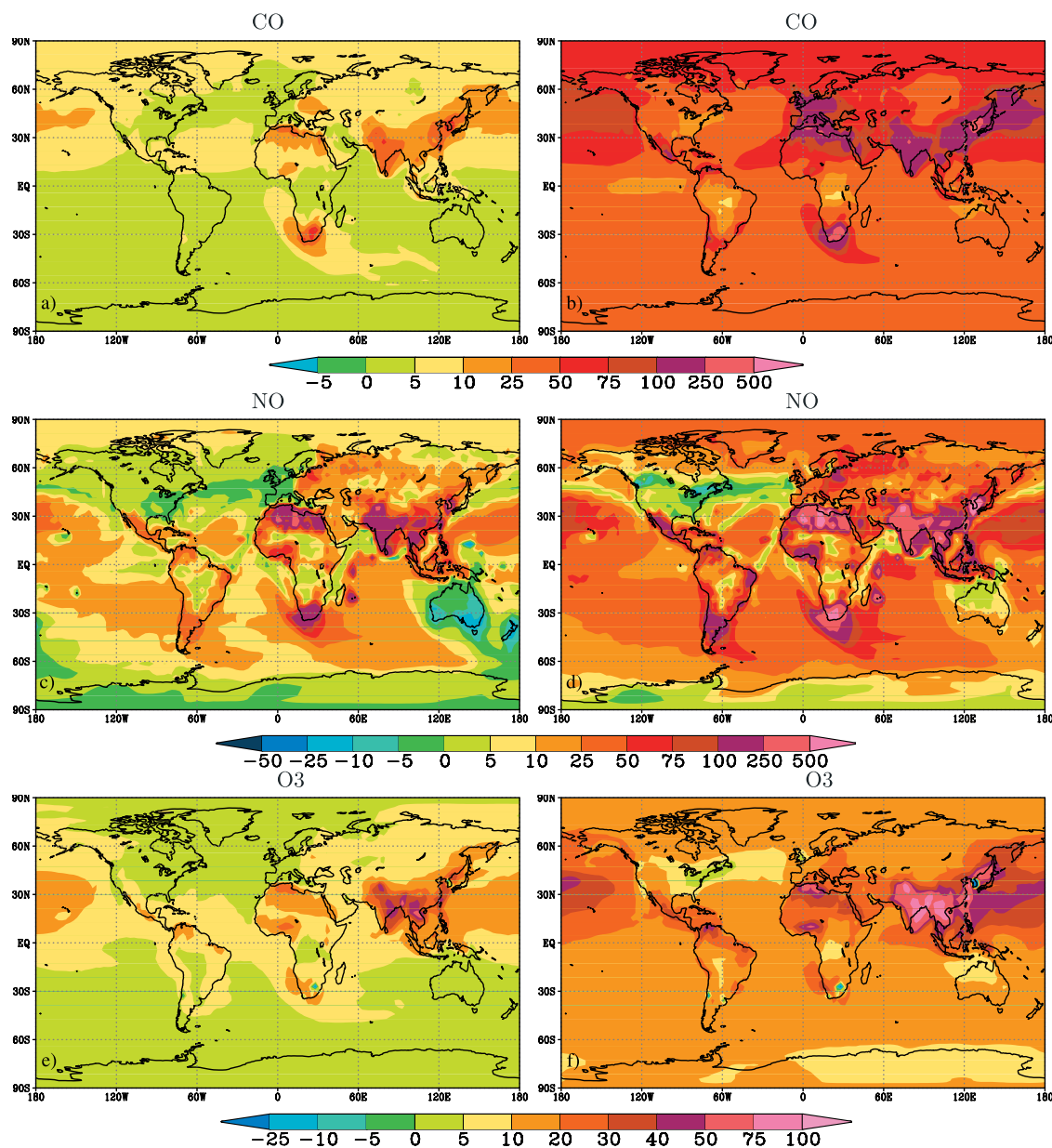
Figure 8. Percentage change in the concentration of (a and b) CO, (c and d) NOx and (e and f) ozone in July between current conditions and a case where traffic emissions are scaled to European per capita traffic emissions (case 5–case 2) (Figures 8a, 8c, and 8e) and a case where traffic emissions are scaled to U.S. per capita traffic emissions (case 6–case 2) (Figures 8b, 8d, and 8f).

15 ppbv, respectively. A plume of enhanced ozone originates in east Asia and extends as far as the islands of Hawaii. In July (see Figure 8f), the calculated increase in the surface ozone concentration at midlatitude and high latitudes reaches 10 ppbv (20%) and 40–50 ppbv (50–100%) in east and south Asia. Near the northern coast of Africa, in eastern Europe, Mexico, South Africa and at some specific areas of South America, the ozone changes are positive, of the order of 10–15 ppbv. A plume of enhanced ozone concentrations, originating in Asia, extends over the North Pacific and reaches the west coast of the United States. The globally averaged radiative forcing due to the ozone changes in response to road traffic emissions under case 6 is 0.27 Wm^{-2} in July and 0.15 Wm^{-2} in January. This repre-

sents approximately 50% of the radiative forcing produced by ozone increase since the beginning of the industrial era.

6. Final Remarks

[46] Model calculations show that the current fleet of road vehicles should have affected significantly the chemical composition of the troposphere, even in remote areas, particularly in the Northern Hemisphere. In the case of ozone precursors including carbon monoxide and nitrogen oxides, the concentration increases most substantially during winter, when photodestruction processes are slow, and the chemical compounds are therefore transported over large distances from the emission sources. The largest increase in the ozone

concentration is predicted to have occurred during summertime, when photochemical activity is highest. The model suggests that, in the Northern Hemisphere, the ozone concentration should have increased by more than 10% in the boundary layer during summertime and by approximately 5–8% during wintertime. At 300 hPa, the traffic-related ozone increase should have been close to 2%. The corresponding globally averaged radiative forcing is approximately 0.05 Wm^{-2} in July and 0.03 Wm^{-2} in January. While slightly increased in July, the level of OH should have decreased in January in the entire Northern Hemisphere in response to surface vehicle emissions. Thus the intensive use of surface vehicles should have somewhat reduced the oxidizing capacity of the atmosphere, and hence increased the lifetime and therefore the atmospheric abundance of compounds like methane with a corresponding increase on radiative forcing.

[47] It is important to stress that the sensitivity of surface ozone concentrations to traffic emissions depends on the level of air pollution by other anthropogenic sources. In order to assess how the effects of current (1997) traffic varies with the concentrations of ozone precursors, we have repeated the calculation (case 2) described in section 5.1, but with anthropogenic emissions of CO and NOx representative of year 2050 (scenario A2P [see *Brasseur et al.*, 2006]), rather than year 1997. As a result of the nonlinearity in the relationship between ozone production and atmospheric nitrogen oxides levels, the calculated increase in surface ozone concentration is substantially less pronounced (approximately a factor of 2) when the background NOx levels are typical of year 2050. This feature is particularly noticeable in industrialized areas where very small automobile-related ozone changes are predicted when the levels of ozone precursors are representative of year 2050.

[48] Finally, it should be emphasized that the focus of this study was on the global effects of traffic, but that local effects (e.g., in urbanized areas), which cannot be properly represented by a global model with limited spatial resolution, could be substantially higher than represented by the present model.

References

Batterman, S., C.-Y. Peng, and J. Braun (2002), Levels and composition of volatile organic compounds on commuting routes in Detroit, Michigan, *Atmos. Environ.*, 36, 6015–6030.

Borrego, C., O. Tchepel, A. M. Costa, J. H. Amorim, and A. I. Miranda (2003), Emission and dispersion modelling of Lisbon air quality at local scale, *Atmos. Environ.*, 37, 5197–5205.

Brandt, J., J. H. Christensen, L. M. Frohn, and R. Berkowitz (2003), Air pollution forecasting from regional to urban street scale-implementation and validation for two cities in Denmark, *Phys. Chem. Earth*, 28, 335–344.

Brasseur, G. P., R. A. Cox, D. Hauglustaine, I. Isaksen, J. Lelieveld, D. H. Lister, R. Sausen, U. Schumann, A. Wahner, and P. Wiesen (1998), European scientific assessment of the atmospheric effects of aircraft emissions, *Atmos. Environ.*, 32, 2327–2422.

Brasseur, G. P., M. Schultz, C. Granier, M. Saunois, T. Diehl, M. Botzet, and E. Roeckner (2006), Impact of climate change on the future chemical composition of the global troposphere, *J. Clim.*, in press.

Brücher, W., C. Kessler, M. J. Kerschgens, and A. Ebel (2000), Simulation of traffic induced air pollution on regional to local scales, *Atmos. Environ.*, 27, 4675–4681.

Buron, J. M., J. M. Lopez, F. Aparico, M. A. Martin, and A. Garcia (2004), Estimation of road transportation emissions in Spain from 1988 to 1999 using COPERT III program, *Atmos. Environ.*, 38, 715–724.

Center for International Earth Science Information Network (2000), Gridded population of the world (GPW), version 2, Columbia Univ., Palisades, N. Y. (Available at http://sedac.ciesin.columbia.edu/plue/gpw).

Colvile, R. N., B. J. Hutchinson, J. S. Mindell, and R. F. Warren (2000), The transport sector as a source of air pollution, *Atmos. Environ.*, 35, 1537–1565.

Granier, C., and G. P. Brasseur (2003), The impact of road traffic on global tropospheric ozone, *Geophys. Res. Lett.*, 30(2), 1086, doi:10.1029/2002GL015972.

Grewe, V., M. Dameris, C. Fichter, and R. Sausen (2001), Impact of aircraft NOx emissions. Part 1: Interactively coupled climate-chemistry simulations and sensitivities to climate-chemistry feedback, lightning, and model resolution, *Meteorol. Z.*, 3, 177–186.

Haagen-Smit, A. J. (1952), Chemistry and physiology of Los Angeles Smog, *Indust. Eng. Chem.*, 44, 1342–1346.

Holzinger, R., B. Kleiss, L. Donoso, and E. Sanhueza (2001), Aromatic hydrocarbons at urban, sub-urban, rural and remote sites in Venezuela, *Atmos. Environ.*, 35, 4917–4927.

Horowitz, L. W., et al. (2003), A global simulation of tropospheric ozone and related tracers: Description and evaluation of MOZART, version 2, *J. Geophys. Res.*, 108(D24), 4784, doi:10.1029/2002JD002853.

Houghton, J. T., Y. Ding, D. J. Griggs, M. Noguer, P. J. van der Linden, and D. Xiaosu (Eds.) (2001), *IPCC Assessment on Climate Change: The Scientific Basis*, 944 pp., Cambridge Univ. Press, New York.

Jacobson, M. Z. (2001), Strong radiative heating due to the mixing state of black carbon in atmospheric aerosols, *Nature*, 409, 695–697.

Köhler, I., M. Dameris, I. Ackermann, and H. Hass (2001), Contributions of road traffic emissions to the atmospheric black carbon burden in the mid-1990s, *J. Geophys. Res.*, 106, 17,997–18,014.

Kristensson, A., C. Johansson, R. Westerholm, E. Swietlicki, L. Gidhagen, U. Wideqvist, and V. Vesely (2004), Real-world traffic emission factors of gases and particles measured in road tunnel in Stockholm, Sweden, *Atmos. Environ.*, 38, 657–673.

Matthes, S. (2003), Globale Auswirkungen des Strassenverkehrs auf die chemische Zusammensetzung der Atmosphäre, dissertation, 160 pp., Univ. München, Munich, Germany.

Matthes, S., V. Grewe, R. Sausen, and G.-J. Roelofs (2005), Global Impact of road traffic emissions on tropopsheric ozone, *Atmos. Chem. Phys. Discuss.*, 5, 10,339–10,367.

Olivier, J. G. J., J. J. M. Berdowski, J. A. H. W. Peters, J. Bakker, A. J. H. Visschedijk, and J. P. J. Bloos (2001), Applications of EDGAR. Including a description of EDGAR V3.0: Reference database with trend data for 1970–1995, *Rep. 773301 001/NRP Rep. 410200 051*, RIVM, Bilthoven, Netherlends.

Olivier, J., J. Peters, C. Granier, G. Pétron, J. F. Müller, and S. Wallens (2003), Present and future surface emissions of atmospheric compounds, *POET Rep. 2*, EU Proj. EVK2-1999-00011. (Available at http://www.aero.jussieu.fr/projet/ACCENT/POET_metadata.php)

Penner, J. E., , D. H. Lister, D. J. Griggs, D. J. Dokken, and M. McFarland (Eds.) (1999), *IPCC Special Report on Aviation and the Global Atmosphere*, 373 pp., Cambridge Univ. Press, New York.

Ramaswamy, V., O. Boucher, J. Haigh, D. Hauglustaine, J. Haywood, G. Myhre, T. Nakajima, G. Y. Shi, and S. Solomon (2001), *IPCC Third Assessment Report*, 350 pp., Cambridge Univ. Press, New York.

Reis, S., D. Simpson, R. Friedrich, J. E. Jonson, S. Unger, and A. Obermeier (2000), Road traffic emissions—Prediction of future contributions to regional ozone levels in Europe, *Atmos. Environ.*, 34, 4701–4710.

Roeckner, E., et al. (2003), The atmospheric general circulation model ECHAM5, part 1: Model Description, *MPI Rep. 349*, 127 pp., Max Planck Inst. for Meteorol., Hamburg, Germany.

Schultz, M. G., J. Feichter, and J. Leonardi (2004), Climatic impact of surface transport, in *Issues In Environmental Science And Technology*, vol. 20, *Transport and the Environment*, pp. 111–127, R. Soc. of Chem., Cambridge, U. K.

Valks, P. J. M., and G. J. M. Velders (2001), The present-day and future impact of NOx emissions from subsonic aircraft an the atmosphere in relation to the impact of NOx surface sources, *Ann. Geophys.*, 17, 1064–1079.

Yamamoto, N., H. Okayasu, S. Murayama, S. Mori, K. Hunahashi, and K. Suzuki (2000), Measurement of volatile organic compounds in the urban atmosphere of Yokohama, Japan, by an automated gas chromotograph system, *Atmos. Environ.*, 34, 4441–4446.

―――――――――――――
G. P. Brasseur and S. Walters, National Center for Atmospheric Research, Boulder, CO 80307, USA.

C. Granier, Service d'Aéronomie/L'Institut Pierre-Simon Laplace, F-75252 Paris, France.

L. Kornblueh and U. Niemeier, Max Planck Institute for Meteorology, D-20146 Hamburg, Germany. (niemeier@dkrz.de)